

# Visualization and analysis of seepage below the dam foundation

---

Šreng, Željko; Kaluđer, Jelena; Šperac, Marija; Miličević, Silvia

Source / Izvornik: **Environmental engineering = Inženjerstvo okoliša**, 2024, 10, 1 - 11

**Journal article, Published version**

**Rad u časopisu, Objavljena verzija rada (izdavačev PDF)**

<https://doi.org/10.37023/ee.10.1-2.1>

Permanent link / Trajna poveznica: <https://urn.nsk.hr/urn:nbn:hr:133:412194>

Rights / Prava: [Attribution-ShareAlike 3.0 Unported/Imenovanje-Dijeli pod istim uvjetima 3.0](#)

Download date / Datum preuzimanja: **2025-04-03**



GRAĐEVINSKI I ARHITEKTONSKI FAKULTET OSIJEK  
Faculty of Civil Engineering and Architecture Osijek

Repository / Repozitorij:

[Repository GrAFOS - Repository of Faculty of Civil Engineering and Architecture Osijek](#)



# VISUALIZATION AND ANALYSIS OF SEEPAGE BELOW THE DAM FOUNDATION

Željko Šreng<sup>1\*</sup>, Jelena Kaluđer<sup>1</sup>, Marija Šperac<sup>1</sup>, Silvia Iva Miličević<sup>1</sup>

<sup>1</sup> Faculty of Civil Engineering and Architecture Osijek

\*E-mail of corresponding author: zsreng@gfos.hr

**Abstract:** The analysis of water seepage below the model's foundation of hydrotechnical object is conducted in the paper. A physical model of gravitational dam is made with the aim to visualize seepage through the ground below the dam. The model is made at the laboratory of the Faculty of Civil Engineering and Architecture in Osijek. The aim of the paper is to analyze the influence of the hydraulic gradient on seepage domain deformation, as well as to study the effect of different engineering measures on the decrease of hydraulic gradient. Four measurements were conducted which were mutually distinguished by the shape of the dam model, i.e. the foundation sheet. The first part of the paper is based on the assessment of measurement variants, i.e. engineering solutions used for the reduction of the seepage part of the buoyancy and seepage flow. The second part of the paper is dedicated to adoption of different models in the analysis of groundwater seepage below the object. Values related to seepage flow as well as buoyancy and pressure distribution below the foundation sheet were analyzed. Graphical, numerical, and approximate methods of analysis were used.

**Keywords:** Seepage flow, Fluidization, Suffusion, Physical model, Numerical model

---

Received: 13.10.2022. / Accepted: 24.01.2023.

Published online: 31.01.2024.

---

Original scientific paper

DOI:10.37023/ee.10.1-2.1

## 1. INTRODUCTION

The path to water is prevented by building a dam on a stream, and accumulation is formed upstream of dam profile with the level of water which is increasing dependent on the dam dimensions and stream valley dimensions. Water held in accumulation attempts to find its way further downstream and overcome the barricade created by dam building. Therefore, the water will probably find its way further below object foundation. In that case it represents a danger and becomes a trigger for different violation mechanisms of dam's general stability. The stress in a body of a dam and its foundation will be affected by the uncontrolled quantity of water which is seeped below the foundation, result of which can be the phenomenon of tensile stresses and crack forming, as well as their later expanding and ultimately, hazard events (Petrović 2002). Moreover, when the flow and seepage pressure values are bigger than the critical values, the groundwater can cause seepage domain deformation which may be dangerous for hydrotechnical construction. The shear strength is decreased by seepage water passing through ground pores affecting the particles to be more apart from one another which is how water penetration is enabled, and potentially a phenomenon of fluidization. The structures should be designed in a way that there is no dangerous seepage deformation such as suffusion, lifting at the contact, seepage uplift, erosion at the contact, sedimentation (Petrović 1997). Mechanical energy per unit of weight of a fluid, i.e. total head, in front of a dam is governing a seepage flow. Therefore, it is a pressure gradient between upstream and downstream side of a dam which affects magnitude of water velocity, not the kinetic energy of the seepage fluid. That principle is integrated into Darcy's law, widely used to quantify laminar groundwater flow:

$$v = -K \cdot grad(H) \quad (1)$$

where  $v$  is the Darcy velocity vector,  $K$  is the hydraulic conductivity coefficient and  $H$  is the total head.

Choosing a suitable place for a foundation of hydrotechnical structures, as well as optimally and rationally determining its shape, design and volume is enabled by understanding the flow and a possibility to quantify the flow with respect to its seepage velocities and seepage flow (Nonveiller 1983). Fluidization downstream of the dam is prevented by decrease of the exit gradient with some of the engineering techniques such as waterproof diaphragm construction below dam's foundation, or prolongation of the seepage path (Savić 2003; Novak 2007) Therefore, in terms of any sort of planning and building of hydrotechnical objects, and in order to choose adequate measures for building protection, it is important to conduct a detailed hydraulic analysis and determine the character of seepage below dam's foundation or through dam's body (Snieder 2004; Jelenković 2013; Luo 2014).

Water seepage below hydrotechnical objects is often regarded as a steady rapidly variable streaming (Petrović 1997). Seepage can be described by the Darcy law due to small water flow velocity and consequently laminar flow. When the shape of a seepage domain is known, as well as initial conditions, i.e. the levels of headwater and tailwater, and with a known hydraulic conductivity coefficient of a seepage domain, it is possible to solve the problem of water seepage through the ground. For the known boundary conditions above mentioned it is necessary to determine potential function  $\Phi(x, y)$  and flow function  $\Psi(x, y)$  which comply with corresponding Laplace's equations:  $\Delta\Phi=0$ ,  $\Delta\Psi=0$ . For the known functions  $\Phi(x, y)$  and  $\Psi(x, y)$ , a hydrodynamic net could be drawn due to which the following values can be obtained: seepage and pore pressure below the dam, seepage flow, seepage force, gradient and velocity. The seepage problem could be solved by applying analytical calculation (those solutions are complex and useless in practice), or by the electrohydrodynamic analogy principle, but also with methods which excludes solving a specific boundary problem of seepage by means of approximate or graphical methods. The use of numerical methods for approximate solving of Laplace's equation with the known boundary conditions is enabled by the development of computer technology. Finite difference method (De Wiest 1969; Bear 2010; Jelenković 2013) and finite element method (Luo 2014; Alzamily 2021) are usually used.

The analysis of water seepage below the model's foundation of hydrotechnical object is conducted in this paper. The aim of the paper is to analyse the influence of the hydraulic gradient on seepage domain deformation, as well as to study the effect of different engineering measures on the reduction of hydraulic gradient. Moreover, 4 different analysis techniques related to seepage problem are adopted in the paper (physical model, approximate method, and numerical model) with the aim for them to be evaluated and compared.

## 2. MATERIALS AND METHODS

### 2.1. Physical method

A physical model related to simulation of seepage through the ground below the foundation was made in the laboratory of the Faculty of Civil Engineering and Architecture in Osijek. The model is built in the device HM 169 which can simulate the conditions of the stationary flow with the help of overflow at inlet and outlet chamber of the device. Moreover, the device is made of a water reservoir from which the water is pumped into inlet chamber from where it enters the experiment tank. The physical model is presented in **Figure 1**. Quartz sand with a uniform grain diameter between 1, 2 and 2 mm was the material used in the seepage analysis. Seepage medium in experiment tank is rectangular with dimension of 120 cm x 30 cm x 15 cm (length x height x thickness). Hydraulic conductivity coefficient of quartz sand is measured as  $0,5\pm 0,12$  cm/s on the permeability/fluidization apparatus. A simplified dam model which is made of the upstream vertical face and foundation sheet is presented in **Figure 1**. The dam model is modular, and its shape can easily be adapted to examination conditions. This means that the length of a foundation sheet as well as the depth of the upstream diaphragm are easily adjustable.

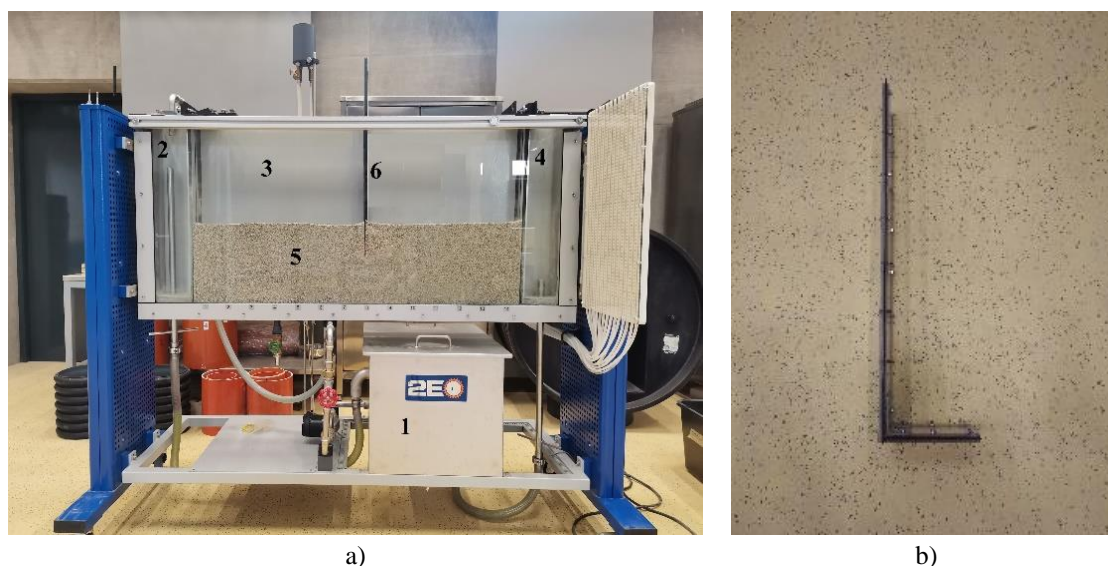


**Figure 1. Physical and dam models: a) physical model (1. water reservoir, 2. inlet chamber, 3. experiment tank, 4. outlet chamber, 5. medium, 6. the dam model); b) the dam model**

Four seepage simulations were conducted below the dam foundation which differed by the length of the impermeable diaphragm ( $S$ ) and the length of the foundation sheet ( $L$ ). The conducted measurements are given in **Table 1** and shown in **Figure 2**. The first measurement ( $S = 2$  cm,  $L = 10$  cm) is used as the backbone of the

experiment, and other variants were compared with respect to it. The goal is to detect and recognize the mechanisms of foundation medium deformation and stability loss (suffusion and uplift of the particles) and conditions under which it takes place (potential difference between upstream and downstream side  $\Delta h$  and critical hydraulic gradient  $I_{cr}$ ). Moreover, seepage flow is measured at the overflow of water into the reservoir (specified by number 1 in **Figure 1**).

**Table 1. Features of the conducted measurements in terms of diaphragm and the foundation sheet**

MEASUREMENT NO.	DIAPHRAGM LENGTH $S$ [cm]	FOUNDATION SHEET LENGTH $L$ [cm]
1	2	10
2	10	10
3	2	15
4	10	15

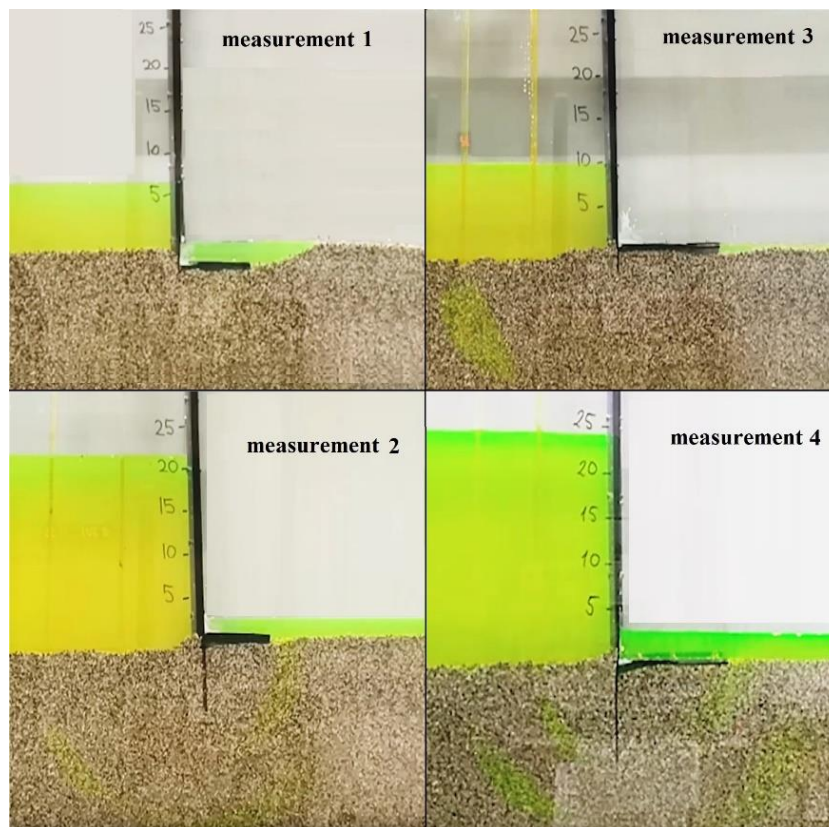


**Figure 2. A display of the conducted measurement; measurement 1 (top left), measurement 2 (bottom left), measurement 3 (top right), measurement 4 (bottom right)**

## 2.2. Graphical method

Graphical method of Laplace's equations comes down to the construction of a hydrodynamic net. It is the orthogonal set of equipotential lines and flowlines. Graphical method of solving the seepage problem is dependent on the experience of the engineer who is designing it. For a more precise hydrodynamic net structure, the fluorescent solution was injected into the physical model. The solution is injected in the upstream side of seepage domain at three points, and in such way three flowlines were obtained. The lines obtained in a such way were used as a landmark related to drawing of hydrodynamic net. Hydrodynamic nets for four variants of measurement that were described in chapter 2.1 are presented in **Figure 3**. Total number of pressure drops  $N_d$  and flow channels  $N_f$  are also specified in **Figure 3**. Dependent on the equipotential distribution it is possible to design distribution of pore pressure below the foundation sheet. Besides pore pressure and seepage pressure, as well as related buoyancy force, by means of a hydrodynamic net, it is possible to determine seepage velocity and flow. When the hydraulic conductivity coefficient and potential drop between two adjacent equipotentials are known, Darcy equation could be applied to get the velocity value. Seepage flow is calculated according to the following:

$$Q = K \cdot \Delta H \cdot \frac{N_f}{N_d} \quad (2)$$

where  $K$  is the seepage coefficient,  $\Delta H$  is the equipotential difference (headwater and tailwater),  $N_f$  is the number of flow channels,  $N_d$  is the number of potential drops.

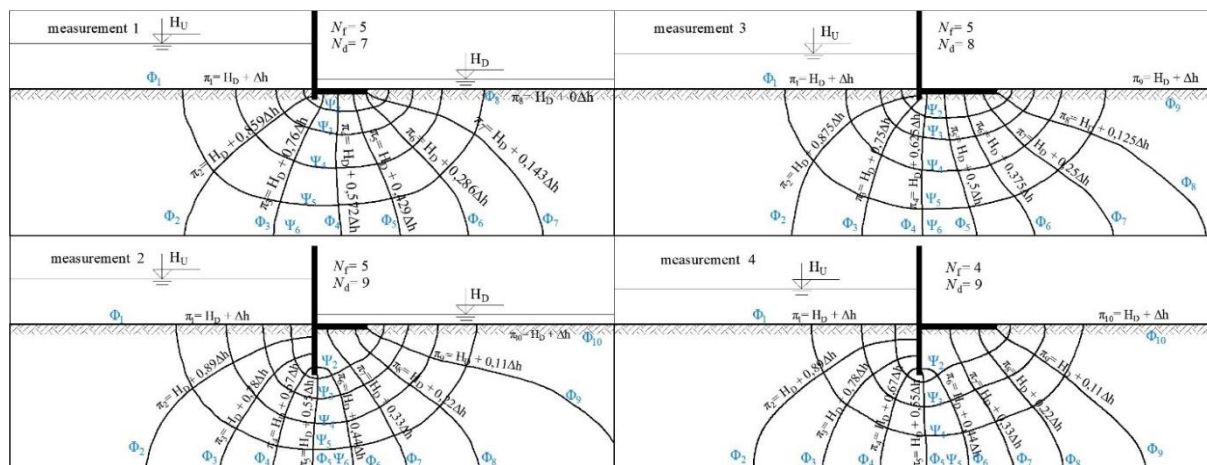


Figure 3. Hydrodynamic net – graphical method; measurement 1 (top left), measurement 2 (bottom left), measurement 3 (top right), measurement 4 (bottom right)

### 2.3. Approximate method

In seepage pressure and buoyancy force calculation the so-called contact line method is used which presupposes linear decrease of seepage pressure ( $\Delta h$ ) along the contact between object's foundation and seepage medium. In calculation the seepage path is given in a way that the lengths of certain foundation segments are put next to each other. The size of seepage domain (depth and length) and resistance on alteration of groundwater flow for certain angle are not accounted for in this method.

### 2.4. Numerical method

Numerical simulation of water seepage below object's foundation is used as a finite element method performed in GeoStudio – SEEP/W software. Software solves the Laplace's partial differential equation for the functions of equipotentials and flowlines. In order to get the conditions equal to those obtained in a physical model, it is necessary to define boundary conditions for seepage domain. Boundary conditions of Dirichlet type are given on the upstream and downstream side of seepage domain. Since stationary flow is simulated, boundary condition of Dirichlet type is characterized by upstream and downstream water level. Boundary condition of Dirichlet type is changed dependent on the analyzed situation. Neumann type of boundary conditions is given on impermeable borders, precisely on the edges of seepage domain and foundation sheet. Default boundary conditions are shown in Figure 4. Seepage domain consists of 508 nodes and 434 mostly squared cells. Triangular cells are designed on the edges of a dam model where the flow of groundwater changes direction.

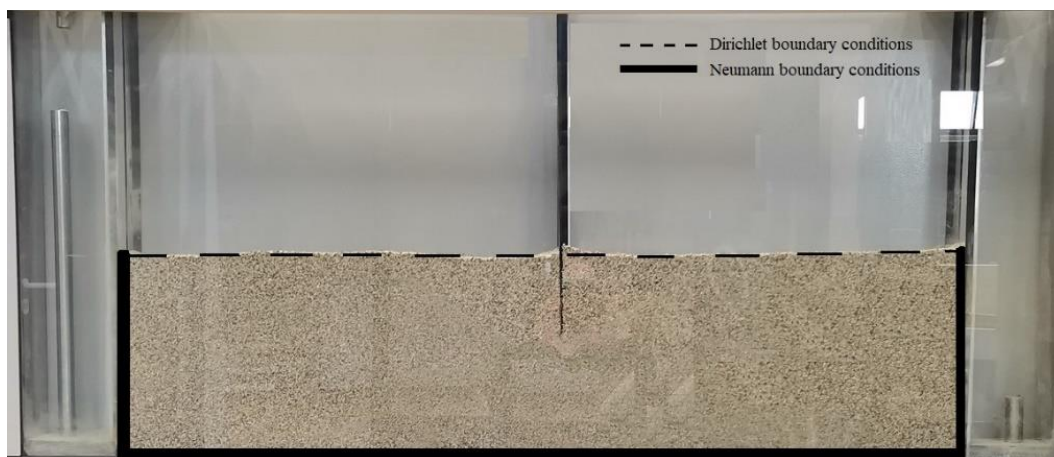


Figure 4. Boundary conditions

### 3. RESULTS AND DISCUSSION

#### 3.1. Physical model

The beginning of the suffusion and sand particle drainage is detected at  $\Delta h = 7$  cm and hydraulic gradient of  $I = 0,46$ . A gradient defined in a such way is compatible with the literary data found in Petrović (1997) where it is stated that the loss of general stability of seepage domain made of coarse-grained sand appears at a critical hydraulic gradient of  $I_{cr} = 0,45$ . Transmission of finer particles is observed through the pores of the coarse ones traveling from upstream to downstream side, as well as upstream funnel formation which was approaching to downstream seepage domain with time. Potential difference of  $\Delta h = 7$  cm is analyzed on remaining 3 measurement variants. Prolongation of the impermeable diaphragm on  $S = 10$  cm is assumed in Variant 2 by which the seepage path is increased, and the hydraulic gradient value is decreased. Variants 3 and 4 are characterized by a longer foundation sheet of  $L = 15$  cm (Table 1). Hydraulic gradient values per measurements are presented in Table 2.

**Table 2. Values of the hydraulic gradient and occurrence of suffusion according to measurements**

MEASUREMENT NO.	POTENTIAL DIFFERENCE $\Delta h$ [cm]	HYDRAULIC GRADIENT $I$ [-]	SUFFUSION
1	7	0,46	YES
2	7	0,22	NO
3	7	0,35	NO
4	7	0,19	NO

It can be observed from Table 2 that the critical hydraulic gradient is in excess only in measurement 1. In measurements 2 and 4 (the impermeable diaphragm with the length of 10 cm) no loss of seepage domain stability is detected, not even in case of a maximum potential difference (due to setup condition) of  $\Delta h = 25$  cm. Although the suffusion did not take place, variants 2 and 4 were also processed in terms of seepage flow and seepage pressure below the foundation sheet for a later comparison with other adopted seepage analyses methods. The phenomenon of suffusion was observed in measurement 3 with the potential difference of  $\Delta h = 10$  cm which is compatible with hydraulic gradient of  $I = 0,5$  ( $> I_{cr} = 0,45$ ). Stability loss mechanism was the same as the one described for the measurement 1. The moment of dragging of soil particles and stability loss of seepage domain is presented in Figure 5.

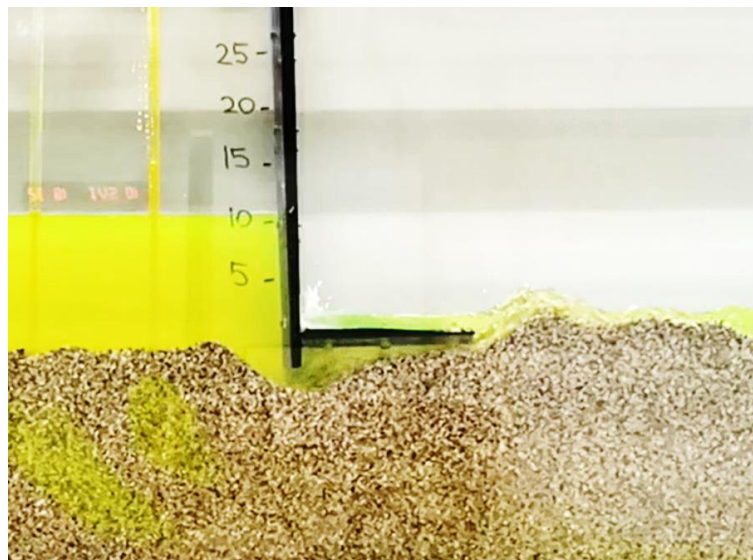


**Figure 5. Deformation of seepage medium at measurement No. 3**

#### 3.2. Graphical method

The designed hydrodynamic net presented in Figure 3 is used for determining seepage pressure distribution as well as seepage part of buoyancy below the foundation sheet. Seepage load diagrams for all 4 measurement variants are presented in Figure 6. Seepage flow value as well as value of seepage part of buoyancy on foundation sheet are presented in Table 3.

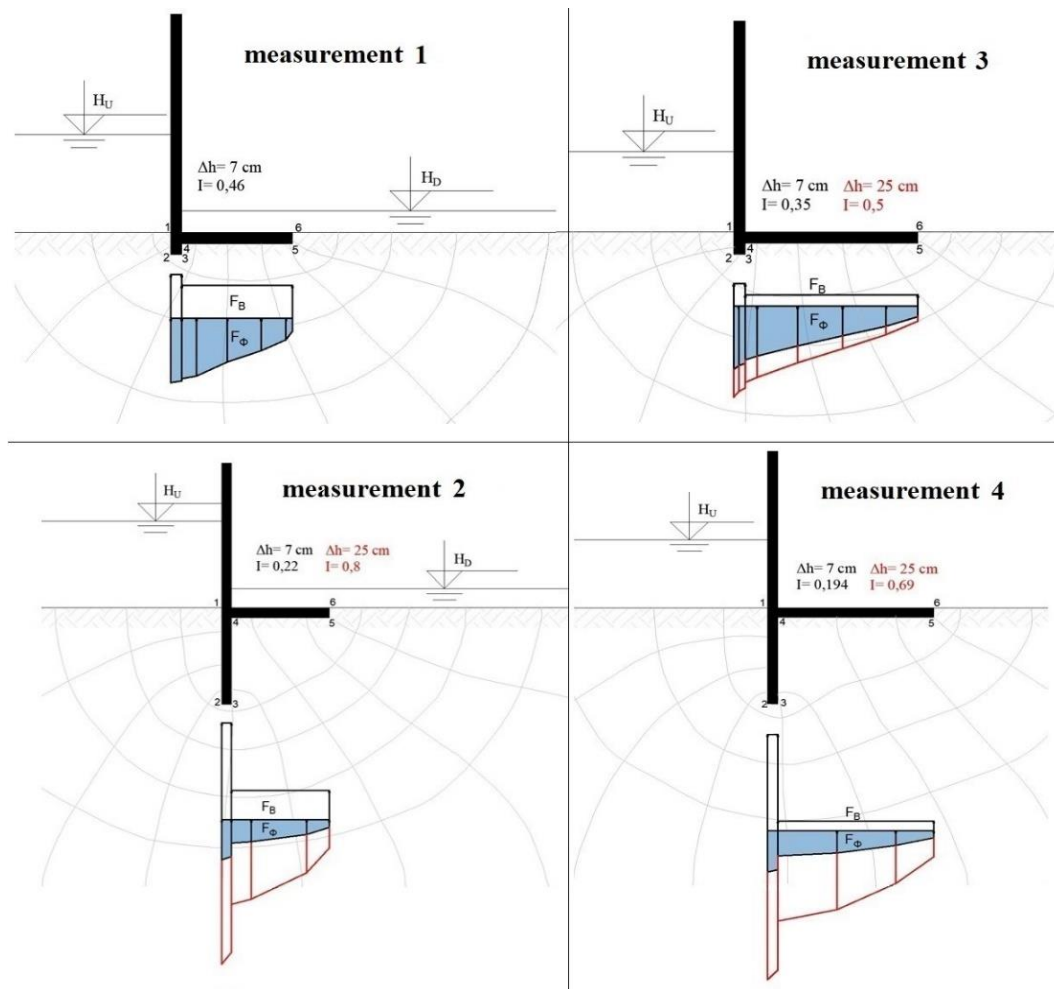


Figure 6. Distribution of seepage and base pressure below the foundation sheet; measurement 1 (top left), measurement 2 (bottom left), measurement 3 (top right), measurement 4 (bottom right)

Table 3. Values of seepage part of buoyancy and seepage flow for conducted measurements

MEASUREMENT NO.	$\Delta h$ (cm)	SEEPAGE FLOW $Q$ [ $10^{-4} \text{ m}^3/\text{s}/\text{m}$ ]	SEEPAGE PART OF BUOYANCY $F_{\Phi}$ [N/m']
1	7	2,5	43,34
2	7	1,94	22,46
	25	6,9	80,22
3	7	2,18	47,76
	10	3,2	68,23
4	7	1,5	32,63
	25	5,55	119,2

It is obvious from the results that flow size is decreased by applying related engineering measures for seepage domain protection. As previously stated, the first measurement was used as a basis, and other situations are evaluated in relation to it. The second measurement which assumed the 10 cm diaphragm was the reason that the flow values were decreased by 22%. It is the result of a longer seepage path during which the groundwater must cross from upstream to downstream side. The longer path will cause the decrease of hydraulic gradient which is proportional with the seepage velocity, and that will consequently cause the decrease of seepage velocity and seepage flow. Graphically speaking (**Figure 3**), the first measurement is characterized by the smallest value of total number of equipotential drops ( $N_d = 7$ ) which is why unit pressure drop ( $\Delta h_i = 0,143\Delta h$ ) and seepage velocity are the biggest values. By looking at the seepage part of buoyancy in the first and the second measurement (**Figure 6**) it is obvious that pressure drop (slope) is smoother in the second measurement, as well as the seepage load surface diaphragm in the second measurement is smaller. Finally, the seepage part of the buoyancy is smaller by 49%. It makes sense that the lower the seepage part of the buoyancy, i.e. the force pushing the flow downstream,

the lower seepage flow and seepage velocity will be. Also, the decrease of seepage flow and the seepage part of the buoyancy is indicated by the results of the third and fourth measurements. As expected, the biggest flow decrease in relation to the 1st measurement is determined in the 4th measurement (40%). Moreover, it is noticed that the diaphragm efficiency in seepage flow and buoyancy reduction is bigger in case of a longer foundation sheet (measurement 3 and 4) in relation to a shorter foundation sheet (measurement 1 and 2).

### 3.3. Numerical model

Vector field of water flux for all 4 measurement variants with  $\Delta h = 7$  cm is illustrated in **Figure 7**. When compared to a physical model, it is obvious that the flowline is concurred with the pathline of the seepage flow which is in accordance with the stationary conditions under which the experiment was conducted. When there was an increase of initial conditions ( $\Delta h$ ) within certain measurement variant, no change in direction and orientation of the flux vector was observed but only in its magnitude. It is evident that the dominant flow direction was the one in the direction of the  $x$  axis when it comes to measurements 1 and 2. Because of the changed geometry of the object foundation there was a change of the vector flux field in measurements 2 and 4. The increase of the flux component in  $y$  direction can be observed which will consequently lead to a decrease of maximum magnitude of water flux. Maximum flux values are presented in **Table 4**. It can be observed that the biggest flux value is in the 1st measurement which is why the suffusion potential as well as stability loss potential is also the biggest in that variant. It is followed by the 3rd measurement while the significantly smaller values of the maximum flux are observed in the 2nd and 4th measurements. The results are in accordance with the observations found in the physical model. In variants 1 and 3 (smaller diaphragm depth) seepage domain stability loss was observed which was not the case with variants 2 and 4. The reason that the suffusion appeared later ( $\Delta h = 10$  cm) in the 3rd measurement is the prolongation of the seepage path by 50% when compared to the 1st measurement. The dominant influence of the flux in  $x$  direction in the 1st and 3rd measurement affected the phenomena of suffusion and dragging of particles right below the foundation sheet (where the velocities are the biggest, **Figure 7**). The biggest flux value is found at places where the groundwater flow abruptly changes its direction (below the diaphragm and on the downstream side of foundation sheet at the exit from the seepage domain), and it is determined by a vector field analysis presented in **Figure 7**. It is the result of the sudden potential drop at those places, which is compatible with the Darcy's law. However, it should be mentioned that although soil particle lift due to exit gradient is not the main stability loss mechanism in the 1st and 3rd measurement, it has surely contributed to a development of the local erosion at the flow exit on the downstream side of the seepage domain.

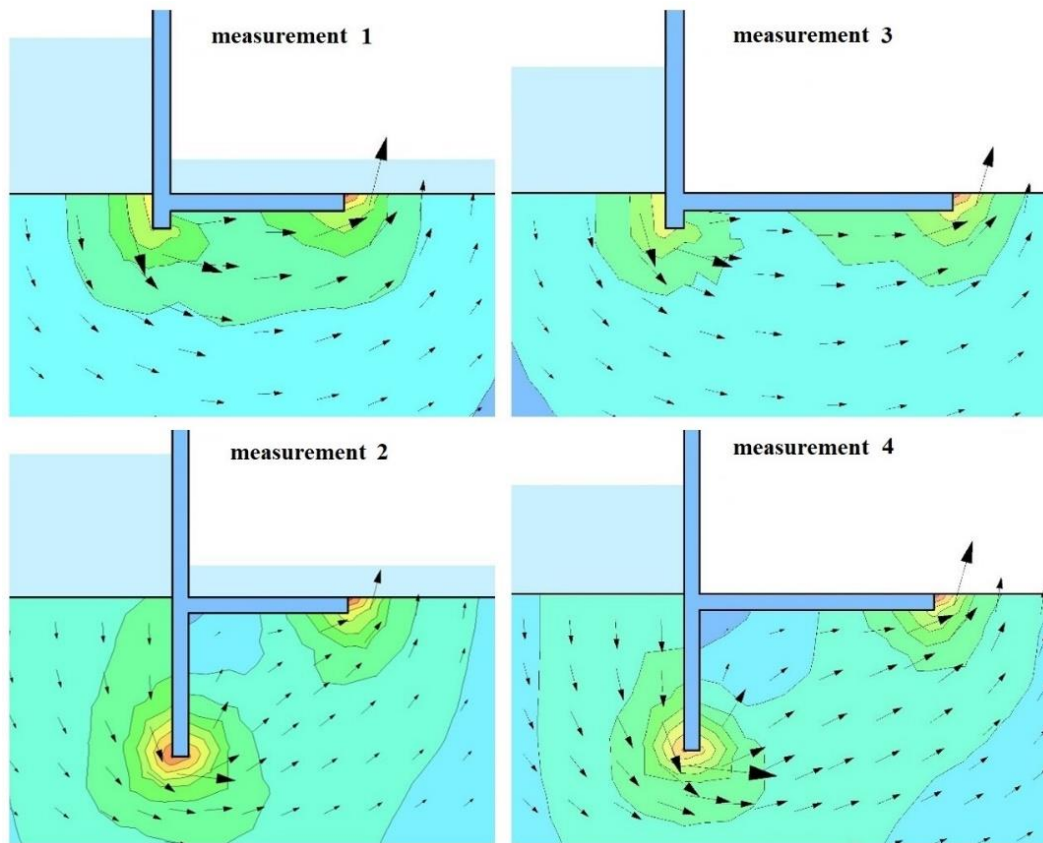


**Figure 7.** Flux vector field below the foundation sheet; measurement 1 (top left), measurement 2 (bottom left), measurement 3 (top right), measurement 4 (bottom right)



**Table 4. Maximum values of water flux for the conducted measurements**

MEASUREMENT NO.	MAXIMUM VALUES OF WATER FLUX $q$ [ $\text{cm}^3/\text{s}/\text{m}^2$ ]
1	0,00459
2	0,0029
3	0,00405
4	0,0029

#### 4. COMPARISON OF METHODS

The comparison of the conducted methods related to analysis of seepage below the foundation sheet is presented in the chapter. The seepage part of the buoyancy and seepage flow were the parameters used in comparison. Diagrams related to the seepage part of the buoyancy for 3 conducted methods are presented in **Figure 8**, while force values are presented in **Table 5**. In the parentheses in the **Table 5**, the deviations of the values in relation to the numerical method are shown. Better congruence of results can be observed in case of graphical and numerical methods in relation to approximate and numerical methods in all the measurements, except for the 3rd. Equipotentials given by numerical and graphical analysis are illustrated in **Figure 9**. When points at which the equipotentials intersect the foundation sheet, it can be observed that the points in the 3rd measurement are differed more than in other measurements (especially in relation to the 4th measurement). As observed from **Table 5**, the value difference between all the analyzed methods is increased with the increase of the initial condition, i.e. potential difference. It is indicated by the results that precise drawing of the hydrodynamic net is important when graphical method is applied, as well as the acceptability of applying graphical and approximate method in determining buoyancy force, especially in initial design phases of hydrotechnical objects.

Seepage flow values are presented in **Table 6** which is indicative of a good congruence of the values obtained by the graphical and numerical method with the flow values obtained on physical model. Almost identical flow values are obtained with graphical and numerical method. The approximate method gives bigger values which is a result of averaging seepage velocity along seepage domain, as well as linear pressure drop along seepage path. In addition, as previously stated, the seepage domain size is not accounted for the method, and to determine seepage flow, some other approximate method would be more applicable, such as resistance coefficient method (Chugaev method).

**Table 5. Values of the seepage part of the buoyancy for conducted measurements and applied methods**

		SEEPAGE PART OF BUOYANCY $F_{\Phi}$ [N/m]		
MEASUREMENT NO.	$\Delta h$ (cm)	GRAPHICAL METHOD	APPROXIMATE METHOD	NUMERICAL METHOD
1	7	54,82 (13,2 %)	42,28 (12,68 %)	48,42
2	7	42,46 (3,38 %)	38,72 (5,72 %)	41,07
	25	100,22 (9,47 %)	84,92 (7,24 %)	91,55
3	7	64,76 (7,2 %)	67,75 (2,92 %)	69,79
	10	85,23 (8,22 %)	89,5 (3,62 %)	92,87
4	7	58,37 (1,3 %)	54,74 (7,47 %)	59,16
	25	143,87 (2,24 %)	131,82 (10,47 %)	147,175

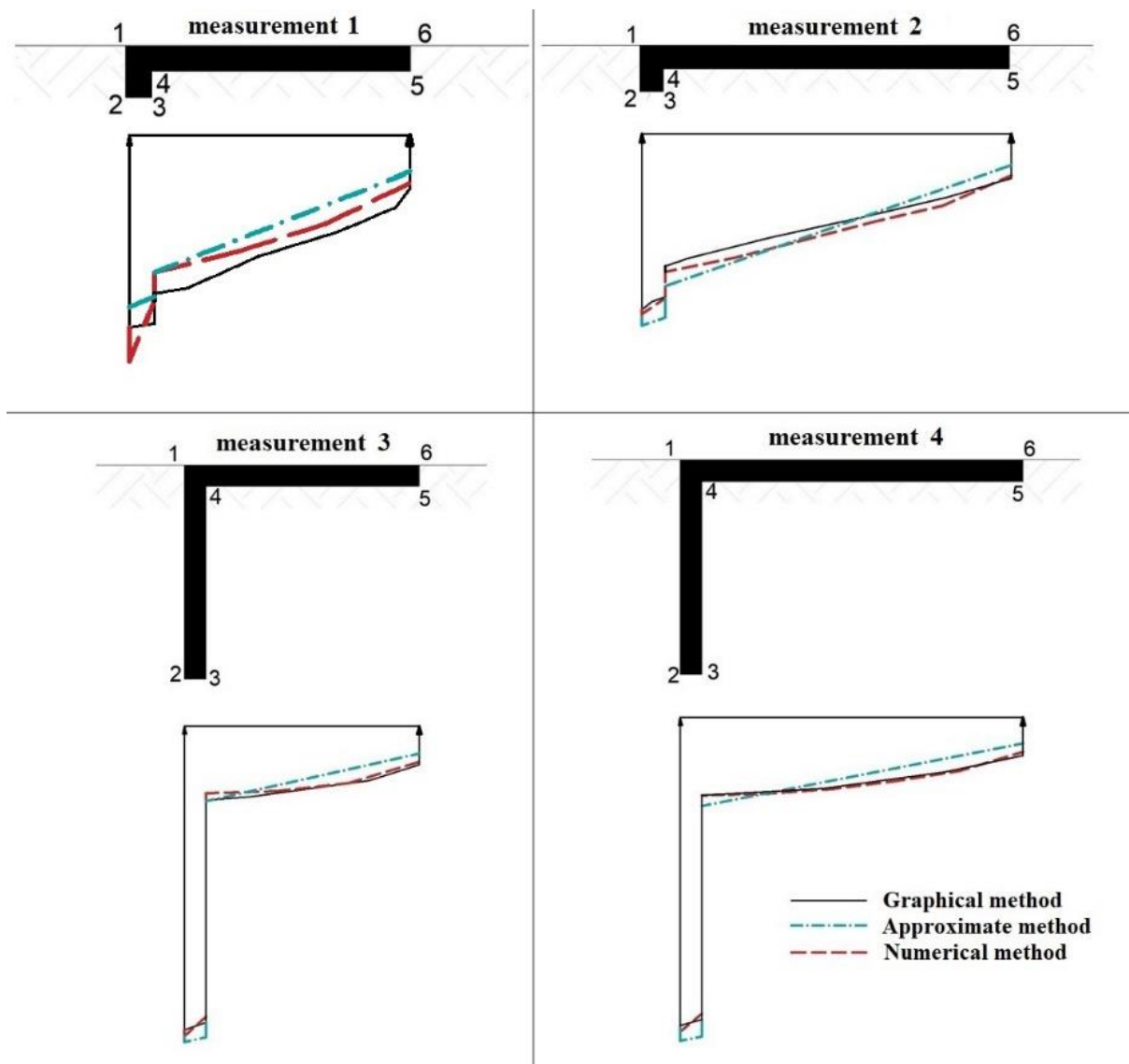


Figure 8. Diagrams of the seepage part of buoyancy according to the applied methods; measurement 1 (top left), measurement 2 (bottom left), measurement 3 (top right), measurement 4 (bottom right)

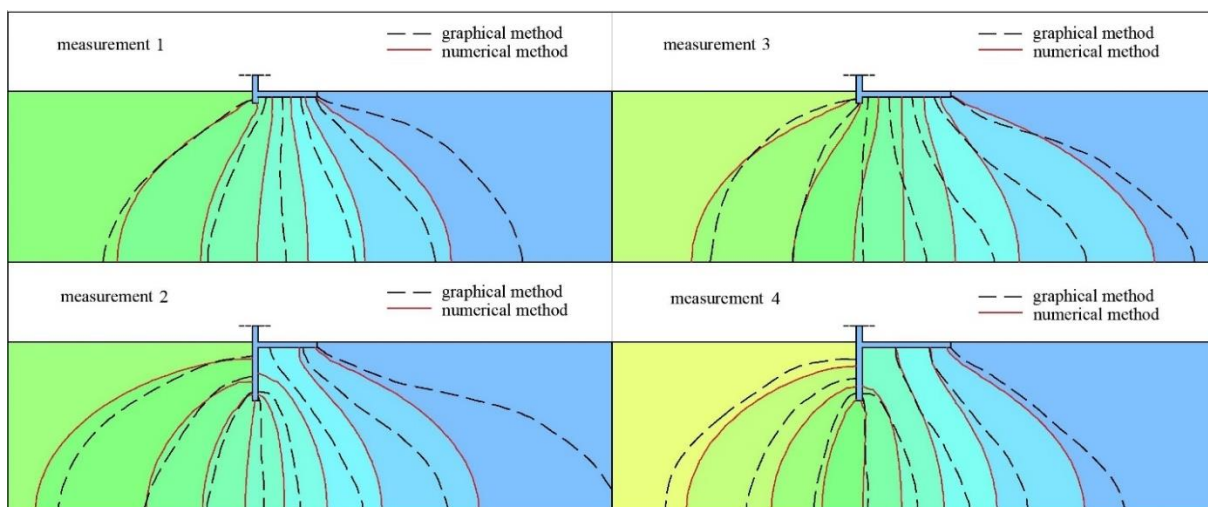


Figure 9. Comparison of equipotentials gained by numerical and graphical method; measurement 1 (top left), measurement 2 (bottom left), measurement 3 (top right), measurement 4 (bottom right)

**Table 6. Values of the seepage flow for conducted measurements and applied methods**

MEASUREMENT NO.	$\Delta h$ (cm)	SEEPAGE FLOW $Q [10^{-4} \text{ m}^3/\text{s}/\text{m}']$		
		GRAPHICAL METHOD	APPROXIMATE METHOD	NUMERICAL METHOD
1	7	2,3	2,5	2,5
2	7	2,1	1,94	1,87
	25	6,7	6,94	6,69
3	7	2,3	2,18	2,2
	10	3,2	3,125	3,152
4	7	1,6	1,55	1,74
	25	5,3	5,55	5,7

## 5. CONCLUSIONS

A physical model for simulation of groundwater seepage below the foundation of hydrotechnical structure is made at the Hydrotechnics Laboratory of the Faculty of Civil Engineering and Architecture Osijek. Stationary water flow through homogeneous, isotropic domain made of quartz sand whose grain diameter of 1,2 to 2 mm is simulated. Four measurements were conducted which were mutually distinguished by the shape of the dam model, i.e. the foundation sheet. The first part of the paper was based on the assessment of measurement variants, i.e. engineering solutions used for the reduction of the seepage part of the buoyancy and seepage flow. The first measurement in which there was no assumed seepage protection such as diaphragm was used as a basis for assessing other measurements. The permanent stability loss of the seepage domain was caused by the phenomenon of suffusion at the point of reaching critical hydraulic gradient. Prolongation of seepage path in a shape of impermeable diaphragm or a horizontal impermeable barrier (in reality, it would be impermeable carpet put upstream of the vertical dam face), has manifested as very efficient in a decrease of buoyancy and flow, result of which was suffusion prevention. A diaphragm which was vertically put below upstream part of the dam has manifested as especially efficient, and its efficiency has increased by the increase of the upstream water level and potential difference.

The second part of the paper was dedicated to adoption of different models in the analysis of groundwater seepage below the object. Values of seepage flow, as well as buoyancy and pressure distribution below the foundation sheet were analyzed. Graphical, numerical and approximate methods of analysis were used. It is indicated by the results that small differences are found in seepage part of buoyancy, as well as that there is a possibility of applying approximate and graphical method in determining the buoyancy force on hydrotechnical object in its earlier design phases. Due to too rough assumptions and simplifications the approximate method provides different results when compared to other methods, so the same as above cannot be said when it comes to seepage flow determination. Very similar solutions, almost identical with the measurements on physical model are provided by the graphical and numerical methods in case of isotropic homogeneous domain.

It is predicted by further research the assessment and comparison of different methods for seepage analysis in non-homogeneous domain below the foundation of the hydrotechnical buildings, but as well as through embankment.

## 6. REFERENCES

- Bear, J., Cheng, A.H.-D. (2010) Modeling groundwater flow and contaminant transport, Springer, Berlin, 2010
- De Wiest, R.J.M., Bear, J. (1969) Flow through porous media, Academic Press, New York
- Jelenković, T., Travaš, V. (2013) numerical and experimental analysis of seepage beneath a model of a gravity dam, Engineering Review Vol. 33, Issue 2, 75-84, 2013
- Luo Y., Zhang, C., Nie, M., Zhan, M., Sheng, J. (2014) An experimental study on embankment failure induced by prolonged immersion in floodwater, Water Science and Engineering
- Nonveiller, E. (1983) Nasute brane – projektiranje i građenje, Školska knjiga, Zagreb
- Petrović, P. S. (1997) Hidrotehničke konstrukcije: Prvi deo. Drugo izdanje. Beograd. Građevinski fakultet Univerziteta u Beogradu
- Petrović, P. S. (2002.) Hidrotehničke konstrukcije: Drugi deo. Beograd. Građevinski fakultet Univerziteta u Beogradu
- Novak, P., Moffat, A.I.B. , Nalluri, C. (2007) Hydraulic Structures: Fourth Edition. Mjesto izdavanja: Taylor & Francis
- Savić, Lj. M. (2003) Uvod u hidrotehničke građevine. Beograd: Građevinski fakultet Univerziteta u Beogradu
- Snieder, R., van den Beukel, A. (2004) The liquefaction cycle and the role of drainage in liquefaction, Granular Matter, 6, 1-9
- Zaid N. Alzamily, Z.N. (2021) Experimental and theoretical investigations of seepage reduction through zones earth dam material with special core, Material Today: Proceedings